Case Study #3: Antibody Fragments in Radiopharmaceutical Therapy

12

Cyprine Neba Funeh, Parinaz Asiabi, Matthias D'Huyvetter, and Nick Devoogdt

12.1 Introduction

Since the approval of Zevalin® in 2002 by the United States Food and Drug Administration (FDA) as the first radiolabeled monoclonal antibody (mAb) for radiopharmaceutical therapy (RPT) of refractory B-cell non-Hodgkin lymphoma, the field of RPT has witnessed remarkable growth, with hundreds of preclinical and clinical trials underway. While mAbs have been explored most often as vectors for delivering lethal payloads to cancer cells, the intrinsic limitations of mAbs as vectors for RPT have fueled interest in other vectors with interesting properties with breakthrough results [1].

An antibody (Ab) or immunoglobulin (Ig) is an affinity protein produced by white blood cells as a key component of humoral immunity, specifically the elimination of pathogens or foreign particles [2]. The efficacy of mAbs is linked with their ability to bind to their targets with high affinity and specificity. Upon binding, they can neutralize the pathogen or function as adaptor molecules which serve an effector function in recruiting other immune cells. In addition to the above-mentioned functions, recombinantly-produced mAbs are harnessed in nuclear medicine as vectors for the delivery of radionuclides to cancer cells for imaging and therapy.

12.1.1 The Structure of an Antibody

There are five different classes of Abs that exhibit diverse functions: IgA, IgD, IgE, IgM, and IgG. IgG is the most abundant of all the Abs (representing ~75% of the total pool of Abs in circulation) and the class commonly used as vectors for RPT. In humans, four subclasses of IgG exist; IgG_1, IgG_2, IgG_3, and IgG_4, each with a specific function [3]. However, the structure of these subclasses is highly conserved. As shown in Fig. 12.1, IgG is a Y-shaped molecule with a molecular weight of about 150 kDa comprised of two identical heavy (H) and light (L) chains. Both the heavy and light chains are in turn composed of constant (C) and variable (V) domains. Each light chain (25 kDa) contains one constant (C_L) and one variable (V_L) domain, while each heavy chain (50 kDa) contains one variable (V_H) and 3 constant (C_H1, C_H2, C_H3) domains. The nature of the heavy chain determines the antibody class and subclass. The two polypeptide chains that make up the Y-shape structure are held together by disulfide bridges at the hinge region and between the C_L and C_H1 domains.

Based on structure and function, mAbs are divided into a Fab region (fragment antigen binding) and an Fc region (fragment crystallizable).

C. N. Funeh · P. Asiabi · M. D'Huyvetter
N. Devoogdt (✉)
Department of Medical Imaging, Laboratory for In Vivo Cellular and Molecular Imaging, Vrije Universiteit Brussel, Brussels, Belgium
e-mail: nick.devoogdt@vub.be

Fig. 12.1 Structure and
different functional
domains of a monoclonal
antibody: Fab region, Fc
region, hinge, light (L) and
heavy (H) chains, variable
(V), and constant
(C) regions
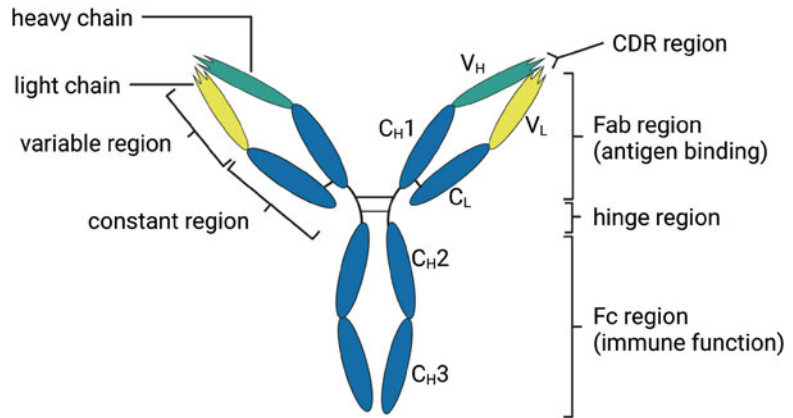
The Fab is made of the variable domains along with C_H1 and C_L, and functions as a region that recognizes and binds to antigens via six hypervariable loops called complementarity determining regions (CDRs), 3 in each variable domain. The Fc region on the other hand is made of the constant domains C_H2 and C_H3, and executes the effector function of mAbs in recruiting immune cells and complement proteins via Fc receptors [2, 3], and regulates the blood half-life of the immunoglobulin through interactions with the neonatal Fc receptor (FcRn). With respect to the latter, the FcRn receptor is found in the endosomes of endothelial cells and monocytes [4]. During circulation, mAbs are taken up via pinocytosis or receptor-mediated endocytosis. Subsequently, FcRn in the endosomes binds to the Fc region of the antibody and protects the Ab from lysosomal degradation. The FcRn-bound Ab then migrates to the cell surface where it is released back into circulation. This mechanism is mediated by changes in pH inside the cell, the low pH of endosomes (pH 6.0) increases the affinity of FcRn for the Fc. Back at the cell surface, the neutral pH (pH 7.0) decreases the affinity of FcRn for Fc, leading to the release of the Ab into circulation [4].

12.1.2 The Concept of RPT

In a key and lock model, an Ab binds to its antigen with high affinity and specificity. This has spurred scientists to generate radiolabeled

mAbs that target membrane proteins that are specifically (over-)expressed on cancer cells. The resulting radioimmunoconjugates are injected into a patient, circulate throughout the body, and specifically bind to their targets expressed on cancer cells. Depending on the radionuclide employed, the emitted particles facilitate either imaging via positron emission tomography (PET) or single-photon emission computed tomography (SPECT), or therapy (RPT). In an approach dubbed "thera(g)nostics," nuclear imaging and therapy are used in conjunction, with the former helping to select patients likely to respond to the latter. Furthermore, when using thera(g)nostic pairs with similar pharmacokinetic profiles (e.g., a single antibody labeled with either a diagnostic or therapeutic radionuclide), imaging can be used to estimate the appropriate radioactive dose for treatment.

12.1.3 Types of Radiations Used in Imaging and RPT

In nuclear medicine, different radionuclides are typically employed for imaging and therapy. For imaging, gamma (γ)-emitting isotopes (e.g., technetium-99 m and indium-111) are used for SPECT, while positron (β^+)-emitting isotopes (e.g., copper-64 and zirconium-89) are used for PET. In contrast, beta (β^-)-emitters (e.g., lutetium-177 and iodine-131), alpha (α)-emitters (e.g., actinium-225 and bismuth-213), and Auger electron-emitters (e.g., gallium-67 and iodine-

125) are used for RPT [5–7]. Therapeutic radionuclides can be differentiated by their decay properties and the linear energy transfer (LET) of the particles they emit. LET is defined as the amount of energy deposited by a particle per unit length along its ionizing track. Simply put, the LET of a particle determines its biological impact on cells: at the same dose, high LET radiation is more toxic than low LET radiation and therefore has a higher likelihood of causing toxicity to healthy tissues if not delivered carefully. Generally speaking, β^--particles exhibit low LET (~0.2 keV/μm), Auger electrons medium LET (between 5–30 keV/μm), and α-particles high LET (from 50–230 keV/μm) [6]. Of note, some radionuclides (e.g., lutetium-177 and iodine-131) emit both γ-rays and β^- particles and are often used in thera(g)nostic applications, as the same radiopharmaceutical can be used for both imaging and therapy [7, 8]. More in-depth examinations of the radionuclides used in RPT can be found in Chaps. 3 and 5.

12.1.4 Radionuclide-Antibody Conjugation Strategies

The selection of a radionuclide and the appropriate bioconjugation chemistry (i.e., bifunctional chelator/prosthetic group and linker) for a radiopharmaceutical should carefully consider the targeting vector to be employed. This is particularly important given that this link can subsequently affect the biological behavior and stability of the compound in vivo. mAb-based radiopharmaceuticals are typically labeled with radionuclides with longer physical half-lives (e.g., zirconium-89) that dovetail with the extended serum residence time of the immunoglobulin [7]. Each mAb has about 30 lysines and about 12 cysteines within their framework which can be exploited to attach radionuclides to the mAb. Depending on the type of radionuclide, a link between the radionuclide and the mAb must be established using a bifunctional chelator or a prosthetic group. For radiometals, a chelator such as diethylenetriamine-pentaacetic acid (DTPA) or tetracyclodecane-tetraacetic acid (DOTA) is often

used [7, 9, 10]. Bifunctional variants of these chelators coordinate the radiometals to prevent their inadvertent release from the conjugate *and* contain moieties that form a stable covalent bond with lysines (or other amino acids) within the targeting vector. In contrast, mAbs can be radiolabeled with radiohalogens like iodine-131 via the direct electrophilic substitution of tyrosine residues within the immunoglobulin. This method is fast, cheap, and straightforward but usually has poor stability in vivo due to deiodination and the subsequent nonspecific accumulation of radioactivity in off-target organs. As a result, more robust radiohalogenation strategies have been developed, including the use of prosthetic groups such as *N*-succinimidyl 4-fluorobenzoate (SFB) and *N*-succinimidyl guanidinomethyl iodobenzoate (SGMIB). In a direct labeling strategy, the antibody is initially pre-modified with a precursor (prosthetic group), followed by the radiolabeling of the immunoconjugate with the radiohalogen of choice. This strategy is frequently used for astatine-211. In an alternative two-step procedure, the prosthetic group is radiolabeled *first* and then conjugated to lysine or cysteine residues within the mAb. Still, more radiohalogenation methods have been developed that harness biorthogonal click chemistry [10].

12.1.5 The Rise of Antibody Fragments for RPT

To date, the use of mAbs as vectors for RPT has proven especially beneficial in the treatment of hematological malignancies, with the approval of Zevalin® (⁹⁰Y-Ibritumomab tiuxetan) and Bexxar® (¹³¹I-tositumomab) for the treatment of refractory non-Hodgkin lymphoma by the US-FDA and European medicines agency (EMA) in the early 2000s [11]. Yet the success of mAbs as vectors for the RPT of solid tumors has remained limited. Both tumor-related factors and the characteristics of the vector play important roles. On the side of the tumor, the dense and fibrous nature of the tumor microenvironment, the availability of the target antigen, and the degree of vascularization of the tumor represent three

prominent factors. The main limiting characteristic of mAbs as vectors stems from their large size and interaction with FcRn, which combine to create a long circulatory half-life that in turn produces myelotoxicity and limits the effective dose that can be safely administered to a patient. Moreover, the large size of mAbs leads to poor tumoral penetration and a heterogeneous distribution within the tumor, rendering them less effective [11]. This is exacerbated by the poor vascularization of solid tumors [1, 13]. A detailed overview of mAbs as vectors for RPT can be found in Chap. 11.

Researchers have explored several strategies to overcome the intrinsic limitations of mAbs, including intra-compartmentalized administration, pre-targeting, and reducing the size of intact mAbs to smaller fragments through recombinant cloning or enzymatic cleavage [1, 13]. In this chapter, we will focus on the latter approach: the use of Ab fragments to build therapeutic radiopharmaceuticals. Indeed, researchers have been able to exploit the structural and functional modularity of IgG to generate smaller, customizable Ab fragments with desirable characteristics as vectors in nuclear medicine [2]. These include Fabs, single chain variable fragment (scFv), single domain antibodies (sdAb), $F(ab')_2$ fragments, diabodies (Db), and minibodies (Mb). In each case, several core properties are altered, including target affinity, tissue penetration, circulatory half-life, and biodistribution [14]. The use of these fragments has opened a new horizon for the treatment of cancer using RPT—especially in the context of solid tumors—as evidenced by a growing number of preclinical and clinical trials. Fig. 12.2 shows a preclinical example of the tumor targeting of radiolabeled sdAbs compared to mAbs.

In the remainder of this chapter, we will explore the use of Ab fragments in RPT. We will examine the need for Ab fragments, describe the pros and cons of each commonly used Ab fragment, describe the production of these probes as well as important preclinical results, and finally explore a handful of clinical trials using fragment-based radiopharmaceuticals.

12.2 The Use of Antibody Fragments in RPT

Ab fragments have several advantages over mAbs as vectors for nuclear medicine. Indeed, the former boast a straightforward production method that makes use of microbial expression systems that are faster, provide high yields, and are cost-effective. Furthermore, due to their small size (ranging from 12 to 110 kDa), antibody fragments can bind to challenging epitopes with cryptic conformations, penetrate deep into tumors, have a shorter serum half-life, and can be cleared faster from circulation through renal or hepatic routes compared to full-length mAb [13]. The lack of a functional Fc domain may also make them safer than mAb-based probes due to the lack of immune-related adverse effects [4].

Despite these clear advantages, it is also important to note that the small size and lack of a functional Fc domain of some Ab fragments can result in low thermostability, increased susceptibility to aggregation, and a shorter half-life due to the absence of FcRn-mediated recycling. Antibody fragments with a molecular weight of less than 65 kDa (the threshold for glomerular filtration) are rapidly cleared from circulation by renal filtration. This rapid clearance of radiolabeled Ab fragments may be associated with their retention in the kidney cortex, a phenomenon mediated by a reuptake mechanism that occurs in the proximal tubuli of the kidneys. Although not yet completely understood, this reuptake mechanism is thought to be mediated by electrostatic interaction between charged patches on the Ab fragments with those on megalin and cubilin receptors in the proximal tubules. In any case, if the retention of the radiolabeled fragments is extensive, it may pose a risk for nephrotoxicity, making the kidneys potential dose-limiting organs for RPT [15, 16]. Several properties of radiolabeled fragments influence the extent of this kidney retention: (i) the presence of charged patches on the structure of the fragment, (ii) the type of radionuclide, and (iii) the bifunctional chelator or prosthetic group used for
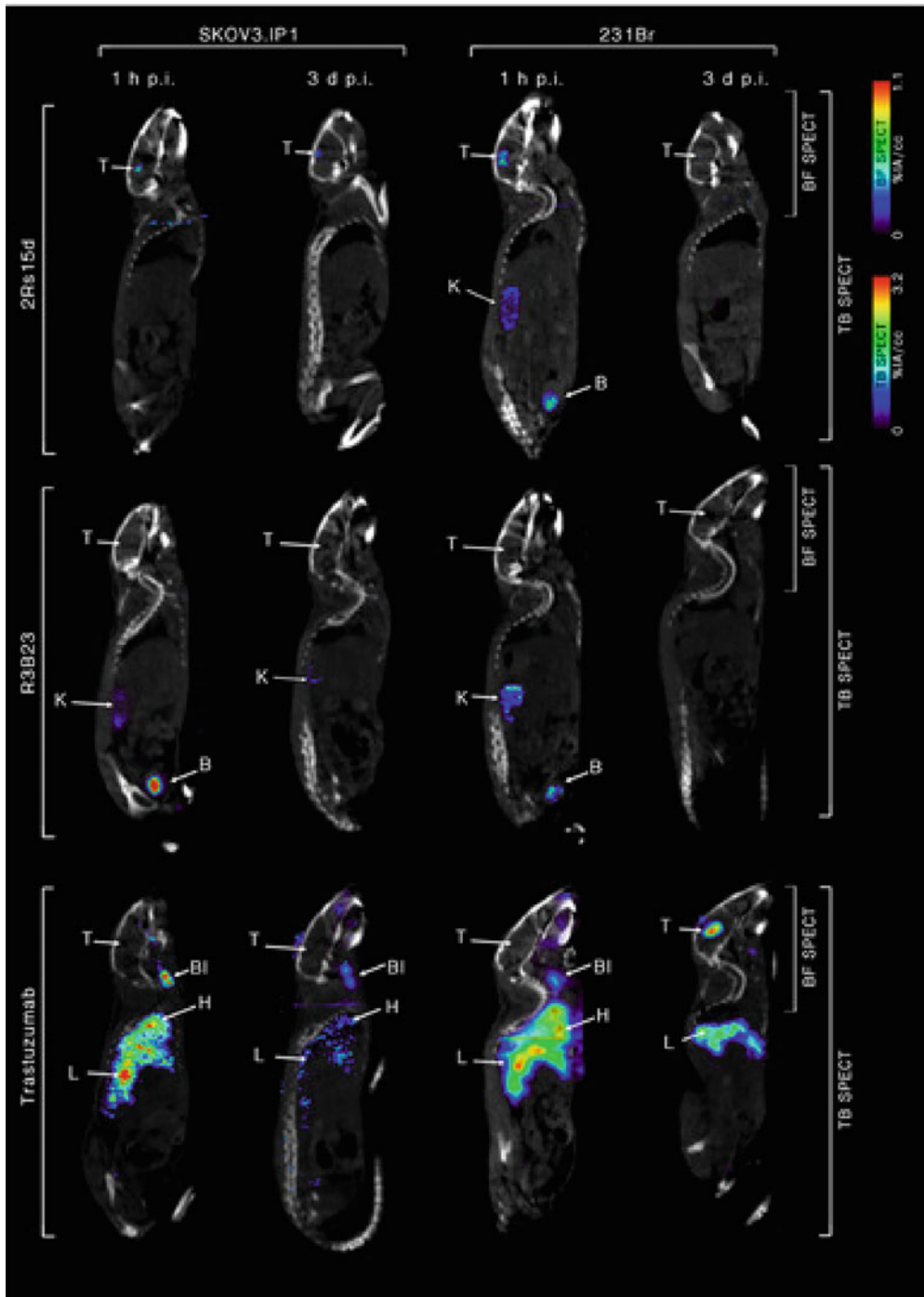
Fig. 12.2 Comparison of the tumor targeting of an ^{111}In-labeled anti-HER2 sdAb, ^{111}In-labeled trastuzumab, and an ^{111}In-labeled control sdAb (R2B23) in the brain metastases of mice bearing SKOV3 and 231Br xenografts. Images taken at 1 h and 3 days post-injection. (Reproduced from J. Puttemans et al., Preclinical targeted α and β⁻ radionuclide therapy in HER2 positive brain metastasis using camelid single domain antibodies; vol 12, 1017; Cancers 2020)

radiolabeling the vectors. For example, radiometals are highly residualized (i.e., trapped within cells) compared to radiohalogens [17]. Also, some prosthetic groups used for radiohalogenation (e.g., SGMIB) have been observed to result in fast-clearing catabolites upon renal filtration, which significantly reduces the renal retention of cytotoxic radiation [18]. A handful of methods have been investigated to reduce kidney retention and are highlighted in the section of sdAbs below. In addition, several methods have been studied to modify the pharmacokinetics of Ab fragments and enhance their circulatory half-life, including multimerization, conjugation with polyethylene glycol (PEG), and the fusion of albumin-binding domains. However, some of these modifications can affect the binding affinity and specificity of the fragments as well as reduce their pharmacokinetic and dosimetric benefits over full-length mAbs [13].

Radionuclides emitting Auger electrons, α-particles, and β$^-$-particles have all been investigated as radionuclides for Ab fragment-based radiotherapeutics. The short circulatory half-life of Ab fragments facilitates the use of short-lived radionuclides that would normally be incompatible with full-length IgG, including astatine-211 ($t_{1/2}$ = 7.2 h), bismuth-213 ($t_{1/2}$ = 42 min), and lead-212 ($t_{1/2}$ = 10.6 h) [7]. Both random and site-specific approaches have been used for the bioconjugation and radiolabeling of Ab fragments [19]. Along these lines, Ab fragments (like mAb) are commonly radiolabeled via conjugation to lysine residues, but the smaller size of the fragments increases the odds that the radiolabeling strategy could interfere with the binding properties of the vector. As a result, the development of site-specific bioconjugation strategies is an area of intense research, as reviewed elsewhere [19]. Table 12.1 highlights the different Ab fragments—including Fab, scFv, F(ab′)$_2$, Mbs, Dbs, and sdAbs—that have been investigated in preclinical and clinical studies for the imaging and RPT of cancer. Due to the promising nature of sdAbs for RPT, they are discussed separately in Sect. 12.3.
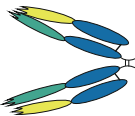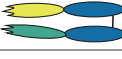
12.2.1 Fab Fragments

In the 1960s, Rodney R. Porter (who later won the Nobel Prize in Medicine in 1972 for his work) demonstrated the possibility of using enzymatic digestion to produce Fab fragments from full-sized mAbs. He showed that these fragments are 3 times smaller than full-size mAbs yet retained the mAb's antigen-binding affinity and specificity at the expense of lower avidity [20]. While affinity is the strength of the interaction between a single Ab binding site (paratope) and a single antigenic epitope, avidity is the combined strength of the interaction between the multiple binding sites of a mAb and the antigenic epitopes. Fab fragments with single binding sites thus tend to have reduced avidities compared to their parental bivalent Ab.

A Fab is a monovalent fragment with a molecular weight of 50–55 kDa [15]. They are the oldest form of Ab fragments used as therapeutics. Initially, they were produced by the enzymatic cleavage of full-sized mAbs using the protease papain [13]. But with advancements in genetic engineering, they can also be recombinantly generated and expressed using bacteria or other expression systems. Structurally, Fab fragments are composed of one light chain (V_L + C_L) along with the variable and constant (V_H + C_H1) domains of a heavy chain. The two chains are linked together by a disulfide bond between the C_L and C_H1 domains to form a monovalent species that retains the binding affinity and specificity of the parent mAb [2, 13]. With a molecular weight 3 times smaller than mAb and the absence of the Fc domains, Fab fragments have numerous advantages as vectors for RPT over mAbs, first and foremost a greatly reduced blood half-life of 12–20 h.
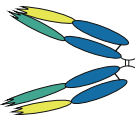
Fab fragments have been proven successful as vectors for RPT in many preclinical studies. For example, a Fab fragment of the mAb nimotuzumab targeting the cancer-associated membrane antigen EGFR was successfully labeled with yittrium-90 (^{90}Y) to obtain [^{90}Y]Y-DOTA-Fab. Subsequently, its biodistribution, specificity, and pharmacokinetic profile were

Table 12.1 Properties, advantages, and disadvantages of various Ab fragments used as vectors in RPT [2, 12, 16, 20, 21]

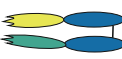| Properties	F(ab')₂	Minibody	Fab	Diabody	scFv	sdAb
Molecular weight (kDa)	110	80	55	55	25	15
Valency	Bivalent	Bivalent	Monovalent	Bivalent	Monovalent	Monovalent
Serum half-life (hours)	8–10	5–10	12–20	5–6	2–4	0.5–1
Mode of production	Enzyme cleavage (papain)	Recombinant (expressed in CHO/HEK cells)	Recombinant and enzyme cleavage (expressed in CHO/HEK cells)	Recombinant (expressed in yeast cells)	Recombinant (expressed in *E. coli* and yeast)	Recombinant (expressed in *E. coli* and yeast)
Route of elimination	Hepatic	Hepatic	Renal	Renal	Renal	Renal
Advantages	Low production cost High overall tumor uptake due to low blood clearance Does not require repeated administration due to low blood clearance Low risk of nephrotoxicity due to low blood clearance and hepatic routes elimination High avidity due to its bivalent construct	High avidity due to bivalent construct High overall tumor uptake due to low blood clearance Low risk of nephrotoxicity due to long blood circulation and hepatic route elimination Does not require repeated administration compared to Fab, scFv, sdAbs Lower propensity for aggregation due to presence of the CH3 domain	Low production cost Rapid blood clearance Deep tumor penetration Rapid biodistribution	Increase avidity due to its bivalent construct Rapid biodistribution Rapid blood clearance Deep tumor penetration	Low production cost Rapid blood clearance Deep tumor penetration Rapid biodistribution	Low production cost and high yield (mg/L) High hydrophilicity Refolding capabilities after chemical or thermal degradation High thermal, pH, and shelf-life stability High affinity and specificity Rapid blood clearance Low immunogenicity due to sequence similarity to human VH Low degree of aggregation Deep tumor penetration Rapid biodistribution Access to hidden epitopes

(continued)

Table 12.1 (continued)

Properties	F(ab')₂	Minibody	Fab	Diabody	scFv	sdAb
						using an extended CDR3 loop. Can be radiolabeled and conjugated with diverse payloads
Disadvantages	Low tumor penetration due to large sizes. Risk of off target irradiation and hematoxicity due to long circulatory half-life. Increased propensity for aggregation	Engineering is time consuming and production yield is low. High production cost. Reduced stability after radiolabeling. Lower tumor penetration relative to scFv, diabody, sdAb and Fab, due to large size	Low overall tumor uptake due to rapid clearance. Risk of nephrotoxicity due to kidney retention. Require repeated administration due to rapid blood clearance. High propensity of aggregation	High propensity for aggregation. Risk of nephrotoxicity due to rapid clearance via the kidney resulting in high renal. Engineering is time consuming. Reduce affinity and stability after radiolabeling. Low overall tumor uptake as a result of rapid blood clearance thus requires repeated administration	High propensity for aggregation. Low overall tumor uptake due to rapid blood clearance. Require repeated administration due to rapid clearance. Risk of nephrotoxicity due to rapid clearance via the kidney resulting in high renal retention. Reduced stability and affinities after radiolabeling	Increased propensity for kidney retention, due to rapid clearance and reabsorption in kidney tubules. Risk of reduce binding affinities after radiolabeling. Therapy requires repeated administration due to rapid clearance

compared to that of [^{90}Y]Y-DOTA-nimotuzumab in normal rats [16]. Higher uptake values in the liver, lungs, and heart were observed for the full-length radioimmunoconjugate compared to the Fab. However, the ^{90}Y-labeled Fab yielded significantly higher accumulation in the kidney compared to the radiolabeled mAb.

12.2.2 F(ab′)$_2$ Fragments

F(ab′)$_2$ fragments are bivalent constructs composed of two Fab fragments joined together at the hinge region by a disulfide bond. They have a molecular weight of approximately 110 kDa and can be generated via the pepsin digestion of a parent mAb [13]. They can also be produced by recombinant methods and expressed in mammalian cells. Though the tissue penetration of F(ab′)$_2$ fragments is reduced compared to that of Fab fragments due to the former's larger size, it is nonetheless superior to that of full-length mAb [13]. The bivalent nature of the F(ab′)$_2$ fragments give them the advantage of increased avidity and retention in tumors, potentially making them more suitable for RPT than Fab fragments. Considering their intermediate size and lack of an Fc region, the blood half-life of F(ab′)$_2$ fragments is longer than that of Fab fragments but shorter than that of full-size mAbs. Furthermore, the molecular weight of F(ab′)$_2$ fragments (110 kDa) is above the 65 kDa cutoff for glomerular filtration, meaning that they are eliminated via the hepatobiliary system and thus exhibit low renal retention. However, the glomerular cutoff of 65 kDa is not an absolute value and is quite an old paradigm. This means that compounds with larger molecular weights have the tendency of being filtered through the kidneys in relatively low amounts compared to smaller molecules. Nonetheless, F(ab′)$_2$ fragments pose a lower risk for kidney irradiation when used as vectors for RPT compared to Fab and scFv. This change is a double-edged sword, however, as the risk of radiotoxicity shifts to the intestines.

F(ab′)$_2$ fragments are the most used fragment in RPT, with numerous preclinical studies and the highest number of clinical trials. Indeed, the only commercially approved fragment-based radiotherapeutic is an ^{131}I-labeled F(ab′)$_2$ fragment of the anti-CD147 mAb metuximab for the treatment of metastatic hepatocellular carcinoma (commercialized as Licartin®). Produced via the pepsin cleavage of parent CD147-targeting mAb HAb18, the ^{131}I-labeled metuximab F(ab′)$_2$ fragment demonstrated a blood half-life of 34.6 h in a pharmacokinetic study in BALB/c mice. In a biodistribution study in murine model of human hepatocellular carcinoma, the absorbed tumor-to-non-target tissue dose ratios of ^{131}I-metuximab F(ab′)$_2$ ranged between 2.5 ± 0.7 and 18.6 ± 2.1. With a 50% effective dose of 370 Mbq/kg for mice and a non-toxic dose of 277.5 MBq/kg in rats, ^{131}I-metuximab F(ab′)$_2$ demonstrated safety and efficacy in targeting hepatocellular carcinoma (HCC). This led to a preliminary clinical study in 9 HCC patients and later a phase I/II trial [21]. After demonstrating these promising efficacy and therapy profiles, the drug was approved by the Chinese FDA for the treatment of metastatic refractory hepatocellular carcinoma [22]. Also, the F(ab′)$_2$ fragment of the mAb chCE7 has been radiolabeled with ^{177}Lu- and ^{67}Cu- for RPT of L1-CAM-expressing tumors [23]. Both radioimmunoconjugates produced higher tumor-to-background activity concentration ratios and lower systemic radiation doses compared to the parent mAb but showed higher renal retention as well. In a therapy study in mice bearing colorectal cancer xenografts, 4 and 8 MBq doses of [^{177}Lu]Lu-DOTAGA-F(ab′)$_2$-cetuximab produced a significant reduction in tumor volume compared to the non-targeting F(ab′)$_2$ control [23].

12.2.3 Single Chain Variable Fragments (scFv)

ScFvs are 25 kDa molecular weight fragments composed of the variable domains of parent heavy and light chains (V$_L$, V$_H$). These chains are genetically linked to each other by a flexible glycine and serine-rich linker [13]. This linker resists protease degradation and allows the fragment to retain a similar specificity and affinity to

the parent mAb [13]. The length of the linker is commonly 12–13 residues and must be individually optimized because it can affect the affinity and stability of the scFv. scFvs are produced by genetic engineering techniques and selected via phage or ribosomal display [16].

Several scFvs have been produced and radiolabeled for the nuclear imaging and RPT of cancer. Haylock et al. [25] generated two scFvs—CD44v6-scFv-A11 and CD44v6-scFv-H12—and labeled these with ^{111}In and ^{125}I for the SPECT imaging of CD44v6-expressing neck and head mouse xenograft tumor models. They observed specific tumor targeting and tumor-to-blood ratios above 5 after 24 h for both the ^{111}In and ^{125}I compounds. At the 48-h time point, the tumor-to-blood activity concentration ratios for the ^{111}In-labeled compounds ([^{111}In]In-DTPA-A11 and [^{111}In]In-DTPA-H12) were greater than 31 (36.9 ± 13.0, 31.6 ± 4.3), while those of the ^{125}I compounds ([^{125}I]I-A11, [^{125}I]I-H12) were greater than 18 (18.2 ± 2.0, 18.9 ± 2.6, respectively) [24]. In another study, Ueda et al., 2015, radiolabeled an anti-HER2 scFv with [^{68}Ga]Ga-desferal for the non-invasive imaging of tumor-bearing mice treated with the chemotherapeutic 17-DMAG. They reported high tumoral accumulation in HER2-positive xenografts and that the imaging helped visualize changes in HER2 expression after therapy. Also, a scFv trimer against CEA was labeled with ^{131}I and evaluated for the treatment of metastatic colorectal carcinoma, ultimately producing convincing enough results to lead a Phase I clinical trial in 2011 [24]. In a cohort of 17 patients, repeated injections of 0.3 mg or 1 mg of radioiodinated CIGB-M3 scFv with activities ranging between 185–259 MBq produced low off-target toxicities coupled with lower immunogenicity compared to patients who received a single dose of 1 mg of a radioimmunoconjugate based on the parental CB-CEA-1 antibody containing the same amount of activity [22]. Although most of the preclinical data with radiolabeled scFvs involve imaging, they have demonstrated good tumor uptake and favorable pharmacokinetics, which increase the likelihood that they can also be radiolabeled with therapeutic radionuclides for use in RPT.

12.2.4 Diabodies (Dbs)

A Db is a bivalent fragment formed when two scFvs are linked together by a flexible linker of about 5–8 amino acids. Dbs are engineered to be either monospecific (two binding sites for the same antigen) or bispecific (two binding sites targeting different antigens). The linker that holds each scFv is shortened so that it prevents the scFv from self-pairing, thereby orienting the two scFvs to form a cross-pair that targets two distinct epitopes in a trans orientation [25]. With a molecular weight of 55 kDa, they have a serum half-life of approximately 5 h. Radiolabeled Dbs have been successfully studied for nuclear imaging and RPT in preclinical studies. For example, a HER2 targeting diabody [^{90}Y]Y-DTPA-C6.5K-A slowed down the growth of breast cancer xenografts compared to non-targeting control [26].

12.2.5 Minibodies (Mbs)

Minibodies—also called small immunoproteins or SIPs—are bivalent, 80 kDa Ab fragments composed of two scFv linked to a C_H3 domain (scFv-C_H3) of IgG. In some cases, however, the scFv is linked to the C_H4 domain of an IgE. The fusion of the scFv to the C_H3 or C_H4 domains is done either via a 2–3 amino acid spacer that forms a non-covalent dimer or via the IgG1 hinge and a flexible linker-peptide that forms a covalent dimer [26]. Mbs are produced by recombinant engineering, are expressed in mammalian cells, and can be engineered to be mono- or bispecific [15]. Unfortunately, Mbs sometimes show decreased thermal stability under clinical conditions due to weak VH-VL interactions. However, some studies have demonstrated that the elongation of the VH-VL linker increases their thermal stability [15].

Mbs have been successfully radiolabeled and studied for both nuclear imaging and RPT. For example, L19-SIP, a Mb targeting fibronectin, was radiolabeled with ^{131}I and evaluated for its therapeutic potential in mice bearing teratocarcinoma tumors. The radiolabeled Mb boasted
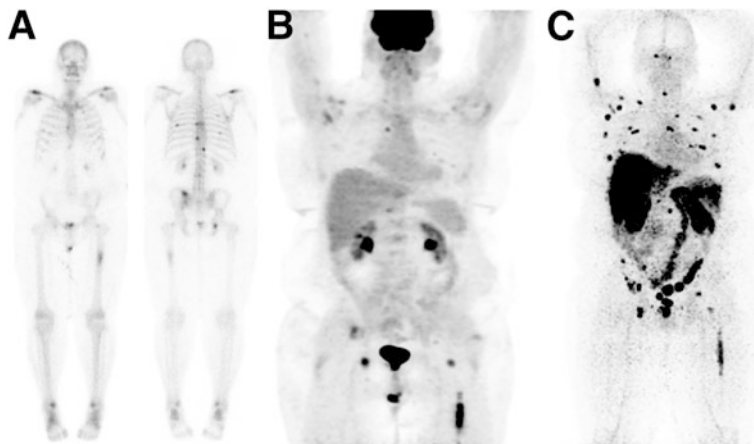
Fig. 12.3 Comparison of the tumor uptake of ^{89}Zr-IAB2M (an anti-PSMA minibody) and ^{18}F-FDG in a patient with metastatic prostate cancer. (**a**) ^{99m}Tc-MDP scans showing uptake in the vertebrae and ribs, (**b**) ^{18}F-FDG PET scans showing uptake in the left femur and low uptake in the vertebral lesions, (**c**) ^{89}Zr-IAB2M SPECT scans showing more uptake in the femur, ribs, and vertebral lesions. (Reproduced with permission from Ref. [27])

superior therapeutic efficacy compared to an analogous ^{131}I-labeled scFv [26]. In addition, a ^{89}Zr-labeled Mb targeting PSMA [^{89}Zr]Zr-DFO-IAB2M was explored for PET in mice bearing prostate cancer xenografts. The promising tumor targeting and the resulting high tumor-to-background contrast prompted the evaluation of the tracer in phase I clinical trial in patients with metastatic prostate cancers (NCT01923727) [27]. No adverse side effects were observed in a cohort of 18 patients, demonstrating the safety of the compound. With an effective dose of 0.41 mSv/MBq, both skeletal and nodal metastasis lesions were detected, and the best visualizations were obtained 48 h after the administration of the radioimmunoconjugate (Fig. 12.3).

12.3   Single Domain Antibodies as Promising Vectors for RPT

One of the most fascinating moments in the last 30 years in the study of antigen binding molecules was the 1993 discovery of single domain antibody fragments (sdAbs) by Hamers et al. [28]. sdAbs are naturally occurring binding domains of heavy-chain-only antibodies (HCAbs) found in the serum of *Camelidae* (alpacas, llamas, dromedaries, camels, guanacos, and vicunas). Compared to conventional antibodies that have two heavy and two light chains, HCAbs have a molecular weight of 95 kDa, consisting of only heavy chains without a C_H1 domain, and possess a single antigen-binding domain in their variable regions called a VHH. The VHH domain is similar in amino acid sequence to the VH domain of human antibodies but contains 3 CDR loops instead of the 6 in Ab-fragments derived from V_H/V_L-containing conventional Abs [29, 30] (Fig. 12.4). This VHH is also called a single domain antibody fragment (sdAb) or a nanobody® (the latter by Ablynx a spin-off company of the Vrije Universiteit Brussel that is now part of Sanofi). SdAbs can be recombinantly produced against almost any antigen. While they typically retain the binding affinity and specificity of their parent antibody, they do (inevitably) exhibit reduced avidity due to their monovalent nature. Finally, sdAbs are the smallest naturally occurring antigen-binding molecule with a molecular weight of 12–15 kDa, a prolate shape with a size of 2.5 × 3 nm, and a serum half-life of 30–60 min.

Fig. 12.4 Structure of a heavy chain only antibody (HCAb) with a single domain antibody fragment [sdAb, also called variable domain of a heavy-chain-only antibody (VHH)]
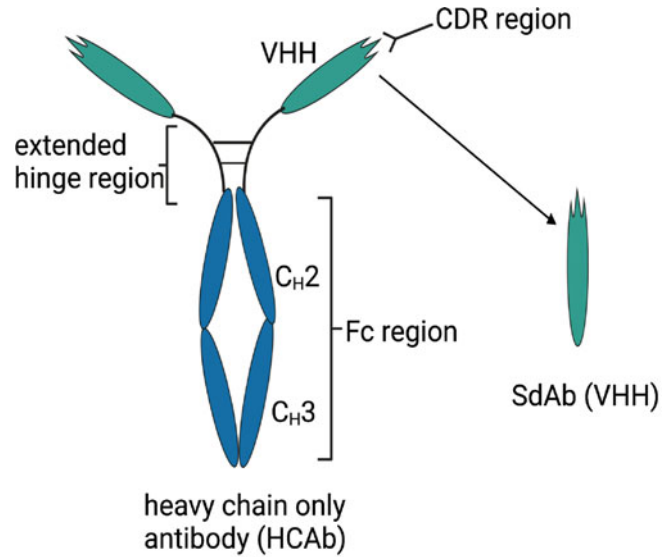
Interestingly, sharks also produce HCAbs called new antigen receptors (NAR) that contain a single antigen-binding domain (V-NAR). Their variable binding domains share some similarities to VHHs, but they differ in structural conformity. Unlike VHHs that share sequence similarities with human VH domains, V-NAR and human VH are much more divergent [30]. To the best of our knowledge, no V-NARs has been investigated for nuclear imaging or RPT.

The increasing interest in the use of sdAbs in diagnostic and therapeutic applications is predicated on their diverse applications and favorable properties. Due to the robustness and versatility of sdAbs, they attracted a lot of attention as potential vectors for RPT. Several sdAbs radiolabeled with therapeutic radionuclides have been preclinically validated with overall good efficacy results and safety profiles. This has led to the approval of some ongoing clinical trials. For example, a radioiodinated sdAb targeting HER2 for the treatment of metastatic brain tumors that express the antigen is currently being evaluated in a multicenter phase Ib/II trial (NCT04467515).

As vectors for RPT, sdAbs are easy and cheap to produce in high yield, and they have high hydrophilicity, making them highly soluble. Furthermore, sdAbs have high thermal, acidic, and shelf-life stability as well as high binding affinity and specificity for their target. Moreover, with a molecular weight of ≈15 kDa, they exhibit a rapid pharmacokinetic profile, penetrate deep into tumors, and are rapidly cleared from circulation through the kidneys. They have a low tendency for aggregation and can be radiolabeled with diverse payloads. Finally, their extended CDR3 loops can access "hidden" antigen epitopes [29]. A detailed example of the preclinical validation and clinical translation of a radiolabeled variant of the HER2-targeting sdAb 2Rs15d for RPT is detailed in a case study in Sect. 12.7.1. The advantages and disadvantages of using sdAbs as vectors for RPT are detailed in Table 12.1.

Preclinical RPT studies with radiolabeled sdAbs have highlighted the risk of nephrotoxicity due to the kidney retention of the radioimmunoconjugates. However, increasing evidence from human trials suggests otherwise [31, 32]. The mechanism of kidney retention of radiolabeled sdAbs is common for all Ab fragments and is explained above. Many mechanisms have been investigated to reduce the kidney retention of sdAbs, including the administration of a solution of positively charged amino acids before and during treatment, the infusion of a plasma expander (gelofusine) [33], and the modulation of the overall charge of sdAbs. Other mechanisms include the

introduction of an albumin-binding domain to the sdAb to slow down its blood clearance and the addition of linkers between the radionuclide and the targeting vector that can be cleaved by kidney brush border enzymes [34]. Using these mechanisms—especially the co-infusion of the radioconjugate with gelofusine—we have previously reported a reduction in kidney uptake by over 40% in preclinical models [33]. In the same study, we observed a 25.1 + 7.3% reduction in kidney uptake when the tracer (^{99m}Tc-7C12) was co-administered with lysine solution, and about a 45% reduction in uptake from the combined co-administration of lysine and gelofusion [33]. In another study, we investigated the effects of the C-terminal polarity of sdAbs on kidney retention. Here, Myc-his-tagged, his-tagged, and untagged ^{111}In-labeled 2Rs15d sdAb ([^{111}In]In-DTPA-2Rs15d) produced kidney uptake values of 52.4 ± 4.7, 36.5 ± 4.3, and 18.2 ± 1.7%IA/g, respectively, in Winster rats [35].

The in vivo cellular and molecular imaging laboratory (ICMI) Brussel has been amongst the pioneers in the use of sdAbs for nuclear imaging and RPT. They have moved three distinct sdAbs (targeting HER2, CD206, and VCAM1) into the clinic through six different clinical trials (NCT03924466, NCT03331601, NCT02683083, NCT04467515, NCT04168528, NCT04483167) for imaging or RPT. Table 12.2 summarizes the different sdAbs that have been preclinically used as vectors for RPT. However, several other sdAbs have been characterized for imaging and could easily be applied to RPT. These imaging studies are described elsewhere [12, 36].

12.4   The Identification of Antibodies and Antibody Fragments

Generally, there are two main methods to generate and identify antibodies and antibody fragments for imaging or RPT. The oldest method relies on hybridoma technology for the production of mAbs that can then be used to generate Fab and F(ab′)$_2$ fragments via enzymatic digestion. After the amino acid sequence of the mAb variable regions is known, recombinant DNA technology can be used to reformat the sequences into smaller fragments that are then expressed in appropriate expression systems (as described in Sect. 12.5). This method is being used to generate Mbs, Dbs, Fab, and scFv. The second method—display technology—involves the selection of individual Ab fragments from large Ab fragment libraries by display technologies and biopanning procedures. This methodology has frequently been used to identify Fab, scFv, and sdAb directly. Recombinant DNA technology can subsequently be used to reformat these fragments into other Ab fragments of interest or even mAbs.

12.4.1   Hybridoma

The development of hybridomas is one of the oldest methods used to generate mAbs. Developed in 1975 by George Köhler and César Milstein, hybridoma technology is based on the fusion of immunized mouse spleen cells with myeloma cells (hybridomas), thereby immortalizing the antibody-producing B lymphocytes. Next, the hybridoma clones are screened via ELISA or flow cytometry to obtain the mAbs with the desired antigen affinity. Hybridomas allow for the production of highly sensitive mAb binders at an affordable cost. Subsequent PCR amplification and sequencing of the V_H and V_L domains of the mAbs identified allow for the generation of Ab fragments via recombinant DNA technology and production in an appropriate host system [37].

There are, however, several drawbacks to using hybridomas to identify mAbs and Ab fragments. First, the process is time-consuming and takes between 6 and 8 months to obtain a reasonable number of mAbs. And second, the murine origin of the mAbs necessitates humanization before translation, which incurs additional costs. In light of these limitations, hybridomas have been progressively replaced by faster and more efficient techniques called display technologies.

Table 12.2 Radiolabeled SdAbs described in preclinical RPT

SdAbs	Target antigen	ERT compound	Disease model
2Rs15d	HER2	[^{131}I]I-SGMIB-2Rs15d	Breast and ovarian cancers (SKOV3-IP1, BT474/M1) (D'Huyvetter et al. 2017, Clin Cancer Res, PMID: 28751451)
		[^{177}Lu]Lu-DTPA-2Rs15d	Breast cancer (D'Huyvetter et al. 2014, Theranostics, PMID: 24883121)
		[^{225}Ac]Ac-DOTA-2Rs15d	Breast and ovarian (SKOV3) (Pruszynski M. et at. 2018, Mol Pharm, PMID: 29502411)
		[^{213}Bi]Bi-DTPA-2Rs15d	Breast (SKOV3) (Dekempeneer et al. 2020, Mol Pharm, PMID: 32787284))
		[^{211}At]At-SGMTB-2Rs15d	Breast (SKOV3) (Dekempeneer et al. 2019, Mol Pharm, PMID: 31268724)
		[^{131}I]I-SGMIB-2Rs15d [^{225}Ac]Ac-DOTA-2Rs15d	HER2$^+$ Brain metastasis (SKOV3-IP1) orthotopic (Puttemans J. et al. 2020, Cancers, PMID: 32326199) HER2$^+$ Brain metastasis (MDA-MB-231Br) orthotopic (Puttemans J et al. 2020, Cancers, PMID: 32326199)
VHH_1028		[^{131}I]I-SGMIB-VHH_1028	Breast and ovarian (SKOV3 & BT474) (Feng Y., Meshaw, R., MacDougald, D. et al. 2022, Sci Rep, doi: 10.1038/s41598-022-07006-9
5F7		[^{211}At]At-SGMIB-5F7 [^{131}I]I-SGMIB-5F7	Breast cancer (BT474-M1) (Choi J et al. 2017, Nucl Med Biol, PMID: 29031230) Breast cancer (B7474-M1) (J Choi et al. 2017 Nucl Med Biol, PMID: 29031230)
1E2 6E10	HGFR	[^{89}Zr]Zr-Df-Bz-NCS-1E2 [^{89}Zr]Zr-Df-Bz-NCS-6E10	Glioblastoma (U87-MG) (Vosjan J.W.D Maria et al. 2012, Mol Cancer Ther, PMID: 22319202)
9079	CD20	[^{177}Lu]Lu-DTPA-9079	Melanoma (human-CD20 transfected B16) (Ertveldt et al. 2022, Mol Cancer Ther, PMID: 35499391)
9079	CD20	[^{177}Lu]Lu-DTPA-9079	Non-Hodgkin lymphoma (Daudi & hCD20$^+$ B16) (Krasniqi et al. 2017, Mol Cancer Ther, PMID : 29054987)
JVZ-007	PSMA	[^{177}Lu]Lu-DTPA-JVZ-007	Prostate cancer (PC295) (Eline A M Ruigrok et al. 2020, Eur J Nucl Med Mol Imaging, PMID: 33094433)
2F8	CD38	[^{177}Lu]Lu-DTPA-2F8	Multiple Myeloma (RPMI 8226) (Duray et al. 2021, J Hematol Oncol, PMID : 34727950)
α-MMR	MMR	[177Lu]Lu-DTPA- αMMR	Mammary adenocarcinoma (TS/A) (Bolli, Evangelia, et al. 2019, J control Release, PMID: 31626860)
mCS-1	CS-1	[^{225}Ac]Ac-DOTA-mCS-1	Multiple Myeloma (5T33MM) (K. DE VEIRMAN et al. 2021, Oncoimmunology, PMID : 34777914)
R3B23	M-protein	[^{177}Lu]Lu-DTPA-R3B23	Multiple Myeloma (5T2MM) (Lemaire M. et al. 2014, Leukemia, PMID : 24166214)

HER2 Human epidermal growth factor receptor 2, *HGFR* Hepatocellular growth factor receptor, *CD20* a cluster of differentiation 20, *PSMA* Prostate-specific membrane antigen, *MMR* Macrophage mannose receptor, *CS-1* Cell surface glycoprotein, *M-protein* Monoclonal protein

12.4.2   Display Technologies

Newer methods for identifying antigen-binding mAbs rely on the screening of Ab-fragment libraries that are displayed on a "selectable" biological entity such as bacteriophage, bacteria, yeast, or ribosomes. The principle of these display technologies is to create a "phenotype/genotype linkage." This means that a displayed Ab-fragment protein is physically connected to a DNA fragment coding for the amino acid sequence of the Ab-fragment. When one selects

a displayed Ab-fragment by an affinity screening (the so-called biopanning procedure), the identity of the Ab-fragment can be easily obtained by sequencing the connected DNA fragment [37].

The most common display technology is phage display. In phage display, *Escherichia coli* bacteriophages are attached to their viral coat an Ab fragment (scFv, Fab, or sdAb), while a DNA fragment that encodes for the Ab fragment is contained within their phage genome (inside the viral coat). The Ab-fragment-displaying bacteriophage is generated by infecting *E. coli* cells that contain Ab-encoding phagemids in their cytoplasm with helper phages. Typically, large Ab-fragment *E. coli* libraries are displayed that contain between 10^6 and 10^{10} different Ab variants. These Ab-fragment libraries are made via the high-throughput DNA cloning of the variable regions of Abs from the B lymphocytes of immunized animals in phagemids and transforming *E. coli* cells (so-called "immune" Ab-fragment libraries). Nowadays, Ab-libraries are made synthetically (i.e., "synthetic" Ab-fragment libraries) without the need for animal immunization by randomizing CDRs of humanized Ab-fragments [37].

The antigen-specific Ab-fragments are selected from these phage-displayed libraries by a "biopanning" procedure. This is an in vitro process of repeated cycles: (i) incubating the phages to bind the Ab-fragment library repertoire to an immobilized antigen; (ii) washing to eliminate the non-specific binders, and (iii) eluting and amplifying to obtain the Ab-fragments that specifically bind to the antigen. This procedure is repeated 2–4 cycles to select the best binders from the library that are then sequenced. The most powerful advantages of phage display are its ease of use, low cost, versatility, and speed (a couple of weeks) [37].

12.5 The Production of Antibodies and Antibody Fragments

E. coli was the first bacterial system used to produce Ab fragments that are not glycosylated.

One-third of approved protein therapeutics by the FDA and EMA are produced by either cytoplasmic or periplasmic *E. coli* expression systems [38]. However, the production of large recombinant proteins containing multiple disulfide bonds in *E. coli* is challenging [39]. These proteins need then to be re-folded after purification, which can be time-consuming, inefficient, and costly. Therefore, the *E. coli* host is used as an expression system only for sdAb, scFv, and Fab. Eukaryotic cells have developed an advanced folding, post-translational, and secretion apparatus which enhances the secretory production of Abs (including full immunoglobulins) compared to bacteria. Yeasts combine the short generation time and ease of genetic manipulation of eukaryotic cells with the robustness and simple medium requirements of unicellular microbial hosts. *Pichia pastoris* and *Saccharomyces cerevisiae* represent the predominant yeast strains used for recombinant Ab fragment production. However, yeast lacks the correct human-type glycosylation for mAb production. While glycosylation is not only essential for the proper folding and biological activity of the Fc domain of the mAb, it also ensures stability in circulation. As a result, mammalian cells which allow human-like glycosylation are currently used to produce mAbs. However, mammalian cells have several drawbacks when it comes to bioprocessing and scale-up, resulting in long processing times and elevated costs. Chinese hamster ovary (CHO) and human embryonic kidney 293 (HEK293) cells are the two most popular mammalian hosts for the production of mAbs and larger Ab fragments such as $F(ab')_2$, minibodies, and diabodies [37, 38].

In addition to recombinant protein expression methods, the production of Ab fragments such as Fab and $F(ab')_2$ can be easily produced from their parent mAb via enzymatic cleavage using commercially available enzymes. While papain cleaves just above the hinge region to produce two Fab fragments and a hinge-C_H2-C_H3 fragment, pepsin cleaves just below the hinge region to produce a $F(ab')_2$ and an Fc fragment [13].

12.6 The Purification of Antibodies and Antibody Fragments

The purification of Ab fragments is more complicated than the purification of full-sized mAbs. This is because of the lack of an Fc domain that facilitates efficient purification by Protein A or Protein G affinity chromatography, which is commonly used for the efficient purification of mAbs. To overcome this limitation, Protein L has been developed and is commonly used for the purification of Ab fragments. Protein L is a cell wall-associated protein isolated from *Peptostreptococcus magnus* that binds strongly to the kappa light chain (V_L) region of certain Ab fragments, such as scFv's, Fab, and sdAbs. Since Protein L interacts with the kappa light chain subtypes, it has no immunoglobulin class restrictions and offers a broadly useful affinity ligand. To extend the usage of Protein L chromatography even further, Protein L has been fused with other Protein G and Protein A, to generate highly versatile affinity ligands with broad binding specificity. This allows it to be used for the purification of Ab fragments containing lambda light chains as well.

At present, Ab fragments are purified using several combinations of chromatographic and non-chromatographic techniques. In light of this, during the production of recombinant Ab fragments, they can be genetically engineered to display affinity tags such as hexa-histidine (6HIS), glutathione-S transferase (GST), or mannose-binding protein (MBP) [40, 41]. These affinity tags offer alternatives to Protein L chromatography and allow for purification via immobilized metal affinity chromatography (IMAC) or other affinity-based methods such as GST-C. However, affinity tags are generally relied upon only for the purification of fragments used in preclinical research. For human applications, affinity tags are rarely included because of the need to remove the potentially immunogenic tags later in production. Instead, secondary chromatography methods are used for purification, such as size exclusion chromatography, ion-exchange chromatography, and mixed-mode chromatography [41].

12.7 The Clinical Translation of Antibody Fragments

While RPT with fragment-based probes has shown great promise in murine models of disease, the successes of Ab fragments as vectors for RPT have not been limited to preclinical studies. Several phases I and II RPT clinical trials with Ab fragments-based radiotherapeutics are underway, as summarized in Table 12.3. As discussed above, one F(ab′)$_2$ fragment-based radiopharmaceutical has received regulatory approval for RPT. Licartin® ([^{131}I]I-metuximab HAb18G) is a pepsin-digested F(ab′)$_2$ fragment of the murine mAb metuximab that targets CD147 and is radiolabeled with iodine-131. It is used for the post-surgical treatment of recurrent metastatic hepatic carcinoma was approved by the Chinese FDA in 2015 [22]. Even though this drug has yet to be approved by EMA and USA-FDA, it nonetheless marks a significant breakthrough for the application of Ab fragments for RPT. At present, most ongoing clinical trials underway involve sdAbs and F(ab′)$_2$ fragments. Indeed, the versatility of sdAbs has fueled increased interest in their use for RPT, and the past decade has witnessed rapid progress in the development and validation of radiotherapeutics based on these fragments. Below we detail the background of the most advanced sdAbcurrently in a clinical trial for RPT.

12.7.1 Case Study: The Clinical Translation of sdAb 2Rs15d for RPT

In 2011, our research group reported the generation and characterization of an anti-HER2 sdAb for non-invasive imaging of HER2$^+$ tumors [42]. The human epidermal growth factor receptor 2 (HER2) is a transmembrane receptor that is overexpressed in about 20–30% of breast cancer patients and at lower frequencies in gastric, ovarian, and colon carcinoma, making it a good target for RPT [35]. This HER2-targeting sdAb, referred to as 2Rs15d, demonstrated highly specific binding to its target with nanomolar

Table 12.3   Different antibody fragments in a clinical trial for RPT of cancer

Fragment	Target	Compound	Trial number	Phase	Status	Disease
2Rs15d	HER2	[^{131}I]I-SGMIB-2Rs15d	NCT02683083	I	Completed	Metastatic HER2$^+$ Breast cancer
2Rs15d	HER2	[^{131}I]I-SGMIB-2Rs15d	NCT04467515	I/II	Recruiting	Metastatic HER2$^+$ breast, gastric, gastro-esophageal cancer
NM-02	HER2	[^{188}Re]Re-NM-02	NCT04674722	I	Recruiting	Breast cancer
MX35 F (ab)$_2$	NaPi2b	[^{211}At]At-MX35 F(ab)2	NCT04461457		Completed	Ovarian cancer
F19SIP Minibody	Fibronectin (domain B)	[^{131}I]I-F19-SIP	NCT01125085	II	Completed	Solid tumor brain metastasis
F16SIP F (ab)$_2$	Tenacin-C	[^{131}I]I-F16SIP (Tenarad)	EudraCT2007-007259-15	I/II	Completed	Refractory Hodgkin's lymphoma
CIGB-m3 ScFv	CEA	[^{131}I]I-CIGB-M3		I	Completed	Metastatic colorectal cancer
HAb18g metuximab F(ab)$_2$	CD147	[^{131}I]I-metuximab HAb18G / CD147 (Licartin$^®$)	ChiCTR-TRC-08000250	P	Completed	Metastatic hepatocellular carcinoma
			NCT00819650	II	Completed	Metastatic hepatocellular carcinoma
			NCT00829465	III	Completed	Metastatic hepatocellular carcinoma
			ChiCTR-TRC-10000837	III	Completed	Metastatic hepatocellular carcinoma

HER2 Human epidermal growth factor receptor 2, *CEA* Carcinoembryonic antigen, *CD147* Cluster of differentiation 147, *NaPi2b* sodium-dependent phosphate transporter 2b, *P* prospective

affinities. Radiolabeled with technetium-99 m, 2Rs15d displayed high tumor uptake and tumor-to-background activity concentrations with limited kidney uptake in a HER2$^+$ mouse tumor model. Furthermore, the binding of 2Rs15d was shown not to compete with the HER2-targeting mAbs trastuzumab and pertuzumab, suggesting the possibility of combination therapies. Due to its targeting potential, 2Rs15d was subsequently radiolabeled with gallium-68 to obtain [^{68}Ga]Ga-NOTA-2Rs15d and preclinically validated for immunoPET in a murine model of HER2-expressing breast cancer [43]. Based on its high tumor-to-background contrast, good tumor-targeting, and lack of toxicity in mice, [^{68}Ga]Ga-NOTA-HER2 was studied in a first-in-human trial evaluating its safety, biodistribution, dosimetry, and targeting potential (Fig. 12.5) [31]. The phase I safety results led to its approval for a phase II trial (NCT03924466) focused on repeatability uptake assessment, whereby its accuracy for the diagnosis of HER2+ breast cancer lesions is assessed by performing repeated

imaging procedures on the same patient. A second phase II trial is evaluating the uptake of the radiotracer in the brain metastases of patients with breast cancer (NCT03331601).

Based on the specific tumor targeting of 2Rs15d, D'Huyvetter et al. labeled the fragment with ^{177}Lu and evaluated its biodistribution, tumor targeting, and therapeutic efficacy in a HER$^+$ mouse tumor model [35]. We observed that the therapy resulted in the efficient blockade of the growth of the HER2$^+$ tumors as well as a significant difference in overall survival compared to a control group. These data opened the door for the preclinical evaluation of RPT with 2Rs15d radiolabeled with other β$^-$- or α-emitters as shown in Table 12.3. For example, we evaluated the biodistribution, therapeutic efficacy, and potential toxicity of 2Rs15d labeled with iodine-131 ([^{131}I]I-GMIB-2Rs15d; CAM-H2) in two HER2$^+$ xenograft mouse models [18]. We observed high tumor uptake that surpassed the kidney accretion levels at 3 h post-administration, low uptake in non-target
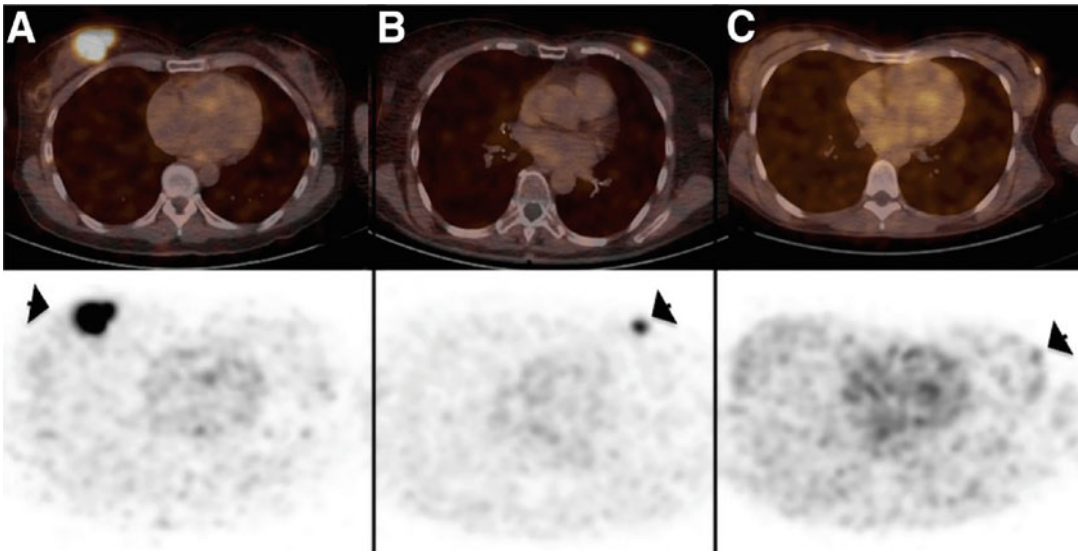
Fig. 12.5 Clinical images (PET/CT: top panel and PET: bottom panel) obtained with a ^{68}Ga-HER2 nanobody in 3 patients with primary breast cancer lesions. (**a**) highest tracer uptake (SUV$_{mean}$,11.8), (**b**) Moderate lesion uptake (SUV$_{mean,}$ 4.9), and (**c**) no uptake (SUV$_{mean,}$ 0.9). (Reproduced from Ref. [31])

organs and tissues, and a significant extension of median survival in the treated mice compared to controls. The preclinical efficacy and safety profile of CAM-H2 led to a first-in-human clinical trial in 2016 (NCT02683083). This phase I trial, which was completed in 2018, evaluated the biodistribution, dosimetry, safety, and tumor imaging of CAM-H2 in 6 healthy adults and 3 patients with metastatic HER2$^+$ breast cancer [32]. The trial data revealed that the radioimmunoconjugate was safe (with no drug-related adverse events in both patients and healthy volunteers), produced focal uptake in metastatic lesions (Fig. 12.6), and was rapidly cleared from circulation via the kidneys.

These results led to the approval of a phase Ib/II clinical trial for CAM-H2 in 2021 (NCT04467515; sponsored by PRECIRIX, formerly known as CAMEL-IDS). This trial is a multicenter clinical trial that evaluates the safety, tolerability, efficacy, and dosimetry of CAM-H2 in 70 patients with metastatic HER2$^+$ breast, gastric, or gastroesophageal junction cancer. This trial is expected to be completed by January 2025. Table 12.3 provides an overview of the various Ab fragments completed or in active clinical trials.

12.8 Conclusion and the Future

In this chapter, we sought to provide insight into the use of Ab fragments for RPT, from preclinical validation to clinical translation to the approval of the first Ab fragment for the RPT of metastatic hepatocellular carcinoma. These fragments have shown great potential as alternative vectors for RPT that overcome many of the limitations of mAbs. All that said, there are still several facets of Ab fragments that remain areas of attention, including their potential for high kidney retention, reduced affinities after radiolabeling, and lower absolute tumor uptake compared to mAbs. We expect that the efficacy and safety of Ab fragment-based radioimmunoconjugates for RPT will increase as interest in these vectors fuels research into novel radiochemical strategies that help optimize their stability and affinity after radiolabeling, and methods to reduce their uptake and retention in the kidneys. In the early 2000s, the clinical translation of Ab fragments for RPT proceeded at a slow pace. However, the recent rise in Ab fragment-based radiotherapeutics entering clinical trials demonstrates hope for the future.
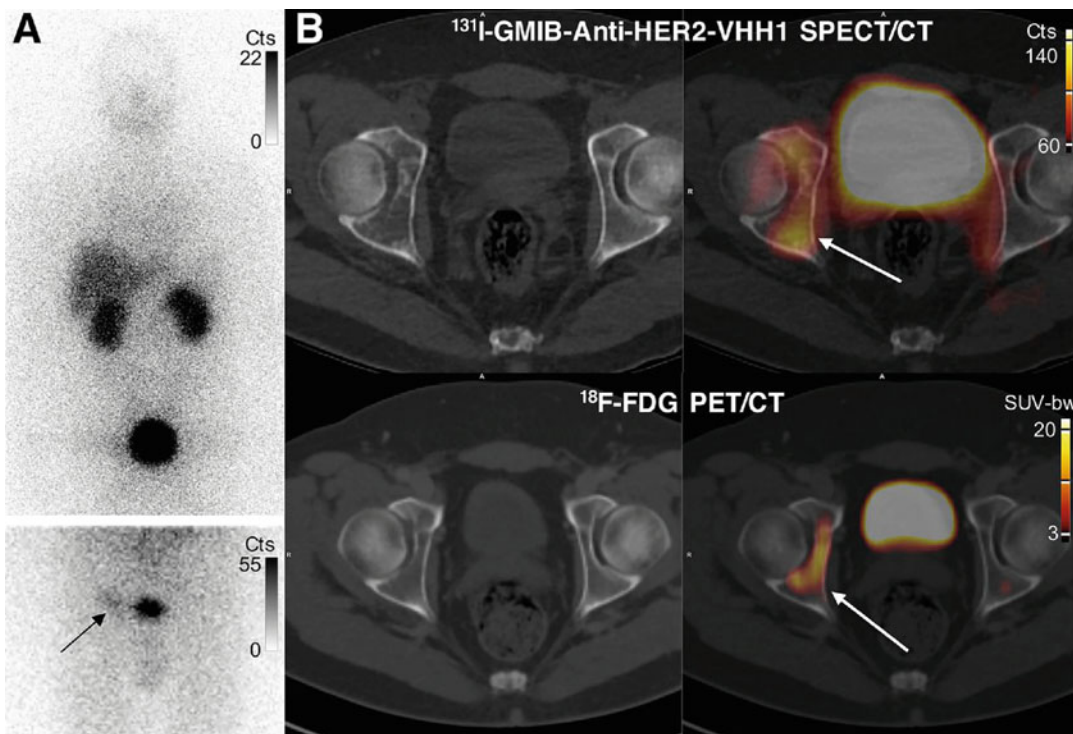
Fig. 12.6 Clinical images of ^{131}I-GMIB-anti-HER2 VHH1 in a patient with bone marrow breast cancer metastasis. (**a**) anterior whole body planar uptake images obtained 2 h post-injection, with the top image showing pronounced bladder activity due to the excretion of the compound and the bottom image depicting a significant drop in activity after urination. (**b**) SPECT/CT (top) and PET/CT images showing increased uptake of the compound in the right acetabular bone at 2.5 h post-injection for ^{131}I-GMIB-anti-HER2 VHH1 and 1-h post-injection for ^{18}F-FDG. *Cts* counts, *SUV-bw* standard uptake value-body weight. (Reproduced from Ref. [32])

12.9   The Bottom Line

- Ab fragments are small (12–110 kDa), maintain antigen affinities similar to that of their parent mAbs, and can be easily, efficiently, and inexpensively generated in microbial expression systems.
- Most Ab-fragments have a short blood half-life, exhibit rapid tumor accumulation, penetrate deep into tumors, and are rapidly eliminated from the body with better safety profiles than full-size mAbs.
- SdAbs have emerged as particularly versatile vectors for RPT, with superior properties compared to other Ab fragments. Several radiolabeled sdAbs have been preclinically validated, and the number of clinical trials with sdAb-based radioimmunoconjugates has increased over the last decade.
- The kidney retention observed after the rapid clearance of low molecular weight Ab fragment-based radioimmunoconjugates (i.e., Fab, scFv, and sdAb) remains a point of attention and poses a risk for nephrotoxicity.
- The past decade has played witness to an increasing number of clinical trials with Ab fragment-based radiotherapeutics, and even more are expected in the coming years.

References

1. Wong KJ, Baidoo KE, Nayak TK, Garmestani K, Brechbiel MW, Milenic DE. In vitro and in vivo pre-clinical analysis of a F(ab′)2 fragment of panitumumab for molecular imaging and therapy of

272 C. N. Funeh et al.

HER1-positive cancers. EJNMMI Res. 2011;1(1):1–15.

2. Alibakhshi A, Abarghooi Kahaki F, Ahangarzadeh S, Yaghoobi H, Yarian F, Arezumand R, et al. Targeted cancer therapy through antibody fragments-decorated nanomedicines. J Control Release. 2017;268:323–34.

3. Tiller KE, Tessier PM. Advances in antibody design. Annu Rev Biomed Eng. 2015;17:191–216.

4. Liu L. Pharmacokinetics of monoclonal antibodies and Fc-fusion proteins. Protein Cell. 2018;9(1):15–32.

5. Maloth KN, Velpula N, Ugrappa S, Kodangal S. Radioisotopes: an overview. Int J Case Rep Image. 2014;5(9):604.

6. Dekempeneer Y, Keyaerts M, Krasniqi A, Puttemans J, Muyldermans S, Lahoutte T, et al. Targeted alpha therapy using short-lived alpha-particles and the promise of nanobodies as targeting vehicle. Expert Opin Biol Ther. 2016;16(8):1035–47. https://doi.org/10.1080/14712598.2016.1185412.

7. Carter LM, Poty S, Sharma SK, Lewis JS. Preclinical optimization of antibody-based radiopharmaceuticals for cancer imaging and radionuclide therapy—model, vector, and radionuclide selection. J Labelled Comp Radiopharm. 2018;61(9):611–35.

8. D'Huyvetter M, Xavier C, Caveliers V, Lahoutte T, Muyldermans S, Devoogdt N. Radiolabeled nanobodies as theranostic tools in targeted radionuclide therapy of cancer. Expert Opin Drug Deliv. 2014;11(12):1939–54.

9. D'Huyvetter M, Aerts A, Xavier C, Vaneycken I, Devoogdt N, Gijs M, et al. Development of 177Lu-nanobodies for radioimmunotherapy of HER2-positive breast cancer: evaluation of different bifunctional chelators. Contrast Media Mol Imaging. 2012;7(2):254–64.

10. Navarro L, Berdal M, Chérel M, Pecorari F, Gestin JF, Guérard F. Prosthetic groups for radioiodination and astatination of peptides and proteins: a comparative study of five potential bioorthogonal labeling strategies. Bioorg Med Chem. 2019;27(1):167–74.

11. Bartholomä MD. Radioimmunotherapy of solid tumors: approaches on the verge of clinical application. J Labelled Comp Radiopharm. 2018;61(9):715–26.

12. Debie P, Lafont C, Defrise M, Hansen I, van Willigen DM, van Leeuwen FWB, et al. Size and affinity kinetics of nanobodies influence targeting and penetration of solid tumours. J Control Release. 2020;317:34–42.

13. Bates A, Power CA. David vs. Goliath: the structure, function, and clinical prospects of antibody fragments. Antibodies. 2019;8(2):28.

14. Xenaki KT, Oliveira S, van Bergen en Henegouwen PMP. Antibody or antibody fragments: implications for molecular imaging and targeted therapy of solid tumors. Front Immunol. 2017;8:1287.

15. Kholodenko RV, Kalinovsky DV, Doronin II, Ponomarev ED, Kholodenko IV. Antibody fragments as potential biopharmaceuticals for cancer therapy: success and limitations. Curr Med Chem. 2019;26(3):396–426.

16. Alonso Martínez LM, Xiques Castillo A, Calzada Falcón VN, Pérez-Malo Cruz M, Leyva Montaña R, Zamora Barrabí M, et al. Development of 90Y-DOTA-nimotuzumab Fab fragment for radioimmunotherapy. J Radioanal Nucl Chem. 2014;302(1):49–56.

17. Chitneni SK, Koumarianou E, Vaidyanathan G, Zalutsky MR. Observations on the effects of residualization and dehalogenation on the utility of N-succinimidyl ester acylation agents for radioiodination of the internalizing antibody trastuzumab. Molecules. 2019;24(21):3907.

18. D'Huyvetter M, De Vos J, Xavier C, Pruszynski M, Sterckx YGJ, Massa S, et al. 131I-labeled anti-HER2 camelid sdAb as a theranostic tool in cancer treatment. Clin Cancer Res. 2017;23(21):6616–28.

19. Massa S, Xavier C, Muyldermans S, Devoogdt N. Emerging site-specific bioconjugation strategies for radioimmunotracer development. Expert Opin Drug Deliv. 2016;13(8):1149–63.

20. Kitten O, Martineau P. Antibody alternative formats: antibody fragments and new frameworks. Medecine/Sciences. 2019;35(12):1092–7.

21. Chen ZN, Mi L, Xu J, Song F, Zhang Q, Zhang Z, et al. Targeting radioimmunotherapy of hepatocellular carcinoma with iodine (131I) metuximab injection: clinical phase I/II trials. Int J Radiat Oncol Biol Phys. 2006;65(2):435–44.

22. Rondon A, Rouanet J, Degoul F. Radioimmunotherapy in oncology: overview of the last decade clinical trials. Cancers. 2021;13(21):5570.

23. Grünberg J, Novak-Hofer I, Honer M, Zimmermann K, Knogler K, Bläuenstein P, et al. In vivo evaluation of 177Lu- and 67/64Cu-labeled recombinant fragments of antibody chCE7 for radioimmunotherapy and PET imaging of L1-CAM-positive tumors. Clin Cancer Res. 2005;11(14):5112–20.

24. Haylock AK, Nilvebrant J, Mortensen A, Velikyan I, Nestor M, Falk R. Generation and evaluation of antibody agents for molecular imaging of CD44v6-expressing cancers. Oncotarget. 2017;8(39):65152–70.

25. Tsai WTK, Wu AM. Aligning physics and physiology: engineering antibodies for radionuclide delivery. J Labelled Comp Radiopharm. 2018;61(9):693–714.

26. Olafsen T, Wu AM. Antibody vectors for imaging. Semin Nucl Med. 2010;40(3):167–81.

27. Pandit-Taskar N, O'Donoghue JA, Ruan S, Lyashchenko SK, Carrasquillo JA, Heller G, et al. First-in-human imaging with 89Zr-Df-IAB2M anti-PSMA minibody in patients with metastatic prostate cancer: pharmacokinetics, biodistribution, dosimetry, and lesion uptake. J Nucl Med. 2016;57(12):1858–64.

28. Hamers-Casterman C, Atarhouch T, Muyldermans S, Robinson G, Hammers C, Songa EB, et al. Naturally

occurring antibodies devoid of light chains. Nature. 1993;363(6428):446–8.

29. Piramoon M, Khodadust F, Jalal S. BBA - reviews on cancer radiolabeled nanobodies for tumor targeting : from bioengineering to imaging and therapy. BBA – Rev Cancer. 1875;2021(2):188529.

30. Muyldermans S. A guide to: generation and design of nanobodies. FEBS J. 2021;288(7):2084–102.

31. Keyaerts M, Xavier C, Heemskerk J, Devoogdt N, Everaert H, Ackaert C, et al. Phase i study of 68Ga-HER2-Nanobody for PET/CT assessment of HER2 expression in breast carcinoma. J Nucl Med. 2016;57 (1):27–33.

32. D'Huyvetter M, De Vos J, Caveliers V, Vaneycken I, Heemskerk J, Duhoux FP, et al. Phase I trial of 131I-GMIB-anti-HER2-VHH1, a new promising candidate for HER2-targeted radionuclide therapy in breast cancer patients. J Nucl Med. 2021;62(8):1097–105.

33. Tchouate Gainkam LO, Caveliers V, Devoogdt N, Vanhove C, Xavier C, Boerman O, et al. Localization, mechanism and reduction of renal retention of technetium-99m labeled epidermal growth factor receptor-specific nanobody in mice. Contrast Media Mol Imaging. 2011;6(2):85–92.

34. Chigoho DM, Bridoux J, Hernot S. Reducing the renal retention of low- to moderate-molecular-weight radiopharmaceuticals. Curr Opin Chem Biol. 2021;63:219–28.

35. D'Huyvetter M, Vincke C, Xavier C, Aerts A, Impens N, Baatout S, et al. Targeted radionuclide therapy with a 177Lu-labeled anti-HER2 nanobody. Theranostics. 2014;4(7):708–20.

36. Harmand TJ, Islam A, Pishesha N, Ploegh HL. Nanobodies as: in vivo, non-invasive, imaging agents. RSC Chem Biol. 2021;2(3):685–701.

37. Arslan M, Karadağ D, Kalyoncu S. Protein engineering approaches for antibody fragments: directed evolution and rational design approaches. Turk J Biol. 2019;43(1):1–12.

38. Ferrer-Miralles N, Domingo-Espín J, Corchero J, Vázquez E, Villaverde A. Microbial factories for recombinant pharmaceuticals. Microb Cell Factories. 2009;8:1–8.

39. Gaciarz A, Khatri NK, Velez-Suberbie ML, Saaranen MJ, Uchida Y, Keshavarz-Moore E, et al. Efficient soluble expression of disulfide bonded proteins in the cytoplasm of Escherichia coli in fed-batch fermentations on chemically defined minimal media. Microb Cell Factories. 2017;16(1):1–12.

40. Spadiut O, Capone S, Krainer F, Glieder A, Herwig C. Microbials for the production of monoclonal antibodies and antibody fragments. Trends Biotechnol. 2014;32(1):54–60.

41. Rodrigo G, Gruvegård M, Van Alstine JM. Antibody fragments and their purification by protein L affinity chromatography. Antibodies. 2015;4(3):259–77.

42. Vaneycken I, Devoogdt N, Van Gassen N, Vincke C, Xavier C, Wernery U, et al. Preclinical screening of anti-HER2 nanobodies for molecular imaging of breast cancer. FASEB J. 2011;25(7):2433–46.

43. Xavier C, Vaneycken I, D'Huyvetter M, Heemskerk J, Keyaerts M, Vincke C, et al. Synthesis, preclinical validation, dosimetry, and toxicity of 68Ga-NOTA-anti-HER2 nanobodies for iPET imaging of HER2 receptor expression in cancer. J Nucl Med. 2013;54 (5):776–84.